Inorganic Chemistry

Article

pubs.acs.org/IC

Oxidation of Bromide to Bromine by Ruthenium(II) Bipyridine-Type Complexes Using the Flash-Quench Technique

Kelvin Yun-Da Tsai and I-Jy Chang*

Department of Chemistry, National Taiwan Normal University, 88 Tingchow Road, Section 4, Taipei 11677 Taiwan

Supporting Information

ABSTRACT: Six ruthenium complexes, $[Ru(bpy)_3]^{2+}$ (**1**), $[Ru(bpy)_2(deeb)]^{2+}$ (**2**), $[Ru(deeb)_2(dmbpy)]^{2+}$ (**3**), $[Ru(deeb)_2(bpy)]^{2+}$ (**4**), $[Ru(deeb)_3]^{2+}$ (**5**), and $[Ru(deeb)_2(bpz)]^{2+}$ (**6**) (bpy: 2,2′-bipyridine; deeb: 4,4′-diethylester-2,2′-bipyridine; dmbpy: 4,4′-dimethyl-2,2′-bipyridine, bpz: 2,2′-bipyrazine), have been employed to sensitize photochemical oxidation of bromide to bromine. The oxidation potential for complexes **1**−**6** are 1.26, 1.36, 1.42, 1.46, 1.56, and 1.66 V vs SCE, respectively. The bimolecular rate constants for the quenching of complexes **1**−**6** by ArN_2^+ (bromobenzenediazonium) are determined as 1.1×10^9, 1.6×10^8, 1.4×10^8, 1.2×10^8, 6.4×10^7, and 8.9×10^6 M^{-1} s^{-1}, respectively. Transient kinetics indicated that Br^- reacted with photogenerated Ru(III) species at different rates. Bimolecular rate constants for the oxidation of Br^- by the Ru(III) species derived from complexes **1**−**5** are observed as 1.2×10^8, 1.3×10^9, 4.0×10^9, 4.8×10^9, and 1.1×10^{10}, M^{-1} s^{-1}, respectively. The last reaction kinetics observed in the three-component system consisting of a Ru sensitizer, quencher, and bromide is shown to be independent of the Ru sensitizer. The final product was identified as bromine by its reaction with hexene. The last reaction kinetics is assigned to the disproportionation reaction of $Br_2^{-\bullet}$ ions, for which the rate constant is determined as 5×10^9 M^{-1} s^{-1}. Though complex **6** has the highest oxidation potential in the Ru(II)/Ru(III) couple, its excited state fails to react with ArN_2^+ sufficiently for subsequent reactions. The Ru(III) species derived from complex **1** reacts with Br^- at the slowest rate. Complexes **2**−**5** are excellent photosensitizers to drive photooxidation of bromide to bromine.

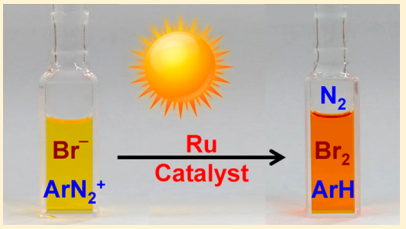

INTRODUCTION

Photochemical reactions take the advantage of photon energy to drive otherwise energetically unfeasible reactions. However, other than energy utilized to overcome reaction barriers, surplus energy generates reactive species that cause undesired reactions. For example, a photoinduced electron transfer (ET) reaction generates potent oxidants and/or reductants that may either cause back ET or side reactions.[1,2] Sacrificial reagents (e.g., EDTA, triethanolamine) have been incorporated to react with one of the photogenerated ET products to avoid the back reaction; however, use of such reagents usually results in low yields.[3−5] Additional, degradation of the photosensitizer may result in low turn-over number (TON).

A flash-quench reaction scheme has been developed to study the long-range electron transfer in biological systems.[6−10] The central concept in the flash-quench technique is to design reactions of the photogenerated species instead of the photoexcited compounds. Thus, the back ET reaction may be suppressed by fast subsequent reactions.

Photochemical splitting of HX to hydrogen and halogen has been demonstrated as a sustainable method for solar energy conversion and storage.[11,12] However, the efficiency of this reaction is often limited by the oxidation of halide to halogen. Although the oxidation of iodide to iodine has been efficiently coupled into photoreaction systems,[13,14] chlorine and bromine productions remain an overwhelming challenge due to high potentials required to oxidize chloride and bromide. Only a few examples have been reported on either stoichiometric or low TON photoproduction of chlorine and bromine with most of them conducted under UV irradiation.[15−19]

Ruthenuim trisbipyridine ($[Ru(bpy)_3]^{2+}$; complex **1**) complex has been widely incorporated in photoinduced electron transfer (ET) reactions. With a suitable redox partner, $[Ru(bpy)_3]^{2+}$ (**1**) easily undergoes ET reactions from its excited state and produces strong oxidants or reductants. Substituents on the bpy ligand shift the redox potentials of the complexes and hence modify the driving forces of the ET reactions.[20] Recently we have reported a visible-light driven, high TON, photocatalytic oxidation of bromide to bromine sensitized with $[Ru(deeb)_2(dmbpy)]^{2+}$ complex (complex **3**).[21] To fully understand the reaction mechanism, we have synthesized four other ruthenium complexes with strong electron withdrawing groups on the bipyridine, $[Ru(bpy)_2(deeb)]^{2+}$ (**2**),[22] $[Ru(deeb)_2(bpy)]^{2+}$ (**4**),[22] $[Ru(deeb)_3]^{2+}$ (**5**),[22] and $[Ru(deeb)_2(bpz)]^{2+}$ (**6**)[23] together with $[Ru(bpy)_3]^{2+}$ (**1**) (Scheme 1), to further investigate the application of the flash-quench technique in the photoproduction of bromine.

RESULTS AND DISCUSSION

Photophysical and Redox Properties of Ruthenium Complexes. The ruthenium complexes prepared in this work exhibit similar absorption and emission spectra, while

Received: May 14, 2017

DOI: 10.1021/acs.inorgchem.7b01238
Inorg. Chem. XXXX, XXX, XXX−XXX

Scheme 1

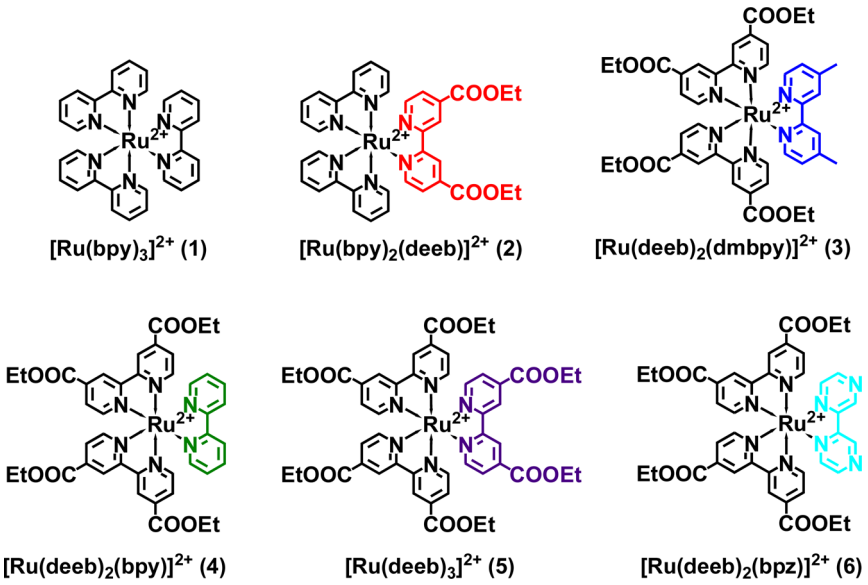

complexes with substituted bpy show red shifts in both absorption and emission bands compared to $Ru(bpy)_3^{2+}$ (Figure 1). It is not surprising that the use of electron-withdrawing ligands tends to afford a smaller HOMO−LUMO gap in these type of complexes.[24] The homoleptic complexes **1** and **5** have sharper metal to ligand charge transfer (MLCT) absorption bands, while heteroleptic complexes have wider peak-to-shoulder separation. The absorption and emission maxima are listed in Table 1. It has been shown that ruthenium complexes with the deeb ligand have much longer lifetimes.[25] The same behavior has been observed in complexes **2**−**6**. Despite the low emission maximum of 668 nm, $[Ru(bpy)_2(deeb)]^{2+}$ has a lifetime of 910 ns. The long-lived excited-state facilitates photoinduced ET reactions.

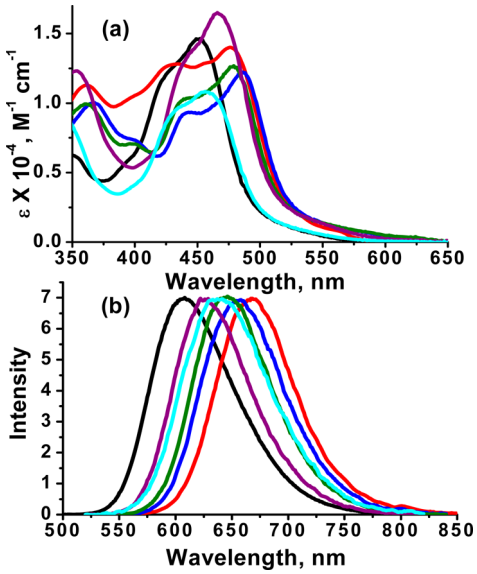

Figure 1. Absorption (a) and emission (b) spectra for complexes **1**−**6** in acetonitrile solution. Complex **1** (−), **2** (red line), **3** (dark blue line), **4** (green line), **5** (purple line), and **6** (light blue line). Emission spectra are not corrected but the intensities are normalized.

Redox potentials, crucial in understanding in ET reactions, were measured for complexes **1**−**6** in acetonitrile solution and listed in Table 1. Cyclic voltammograms of all complexes (Figure 2) exhibit one oxidation and three reduction peaks. The oxidation process has been assigned to the oxidation of Ru(II) to Ru(III). The higher oxidation potentials for complexes **2**−**6** in comparison to $[Ru(bpy)_3]^{2+}$ indicate electron-poor character at the metal centers of **2**−**6** due to the coordination of the strong electron withdrawing deeb ligand. Complex **6**, $[Ru(deeb)_2(bpz)]^{2+}$, judged to bear the highest electron-withdrawing effect of the ligands exhibits the highest oxidation potential (1.66 V vs SCE) among these sensitizers. The reduction potentials were assigned to the ligand reduction processes. Each diimine ligand is capable of one electron reduction; therefore, three reduction peaks are observed. For the homoleptic complexes **1** and **5**, the reduction potential increases about 0.2 V for each further reduction, though at very different potentials. The first reduction potential of complex **5**,

Table 1. Absorption and Emission Maxima, Lifetime, and Redox Potentials for Complexes 1−6 in Acetonitrile Solution

	$[Ru(LL)]^{2+}$, LL =	λ_{abs}, nm (ε, 10^4 M^{-1} cm^{-1})	λ_{em}, nm	τ, ns	$E_{1/2}(Ru^{III/II})$[a], V	$E_{1/2}(Ru^{2+/+})$[a], V	$E_{1/2}(Ru^{+/0})$[a], V	$E_{1/2}(Ru^{0/-})$[a], V
1	$(bpy)_3$	451 (1.46)	608	740	1.26	−1.36	−1.55	−1.78
2	$(bpy)_2(deeb)$	476 (1.40)	668	910	1.36	−1.02	−1.47	−1.68
3	$(deeb)_2(dmbpy)$[b]	486 (1.22)	656	1130	1.42	−0.96	−1.15	−1.63
4	$(deeb)_2(bpy)$	478 (1.26)	645	1400	1.46	−0.96	−1.15	−1.59
5	$(deeb)_3$	466 (1.65)	626	2020	1.56	−0.91	−1.06	−1.27
6	$(deeb)_2(bpz)$	456 (1.08)	637	1050	1.66	−0.84	−1.06	−1.27

[a]Potentials are vs SCE. Electrolyte: 0.1 M Bu_4NBF_4. [b]Ref 21.

DOI: 10.1021/acs.inorgchem.7b01238
Inorg. Chem. XXXX, XXX, XXX−XXX

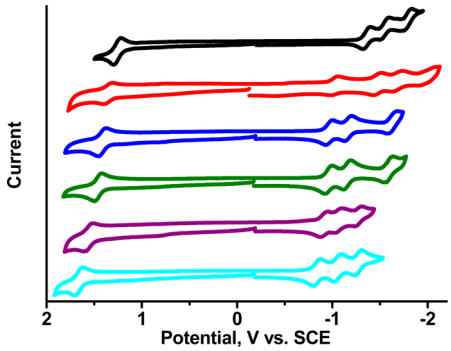

Figure 2. Cyclic voltammogram of complexes **1**–**6** (from top to bottom) in acetonitrile solution. Standard three component cell that consists of a glassy-carbon (3 mm^2) working electrode, Pt and Ag wires as counter and reference electrodes, respectively, are utilized. Tetrabutylammonium tetrafluoroborate (0.1 M) is utilized as the supporting electrolyte. Scan rate is 100 mV/s. Potentials are obtained from separate scans with ferrocene as the internal standard.

$[Ru(deeb)_3]^{2+}$, shows a substantial anodic shift relative to complex **1**, $[Ru(bpy)_3]^{2+}$. These well-separated reduction processes indicate that the electron is localized on individual ligands, and each ligand reduction makes the further ligand reduction harder. For heteroleptic complexes, three reduction potentials show one large and one small gap. It is helpful to assign the site of reduction based on these peak-separation tendencies. For example, it is conclusive that the first reduction for complex **2** and the first two reduction for complex **4** are the reduction of deeb, while the subsequent peaks for complex **2** and the last reduction for complex **4** are the reduction of the bpy ligand. The first reduction potential of −0.84 V for complex **6** confirms that bpz is the ligand possessing the highest electron-withdrawing effect employed in this study. The electron-withdrawing effect decreases in the order of bpz, deeb, bpy, and dmbpy.

Generation of Long-Lived Ru^{3+} by Using 4-Bromobenzenediazonium Tetrafluoroborate (ArN_2BF_4). To produce long-lived Ru^{3+} species, an irreversible oxidative quencher of 4-bromobenzenediazonium tetrafluoroborate (ArN_2BF_4) was utilized.[26,27] The absorption spectra of ground-state ruthenium complexes with various concentrations of ArN_2^+ exhibit no change at all. Upon irradiation, the emission intensity and the lifetime decrease as the concentration of quencher are increased, as shown in Figure 3a. The Stern–Volmer equation (eq 1) is generally utilized to describe the linear relationship of emission intensity and lifetime versus quencher concentration.

$$I_o/I = \tau_o/\tau = 1 + k_q\tau_o[Q] \quad (1)$$

A Stern–Volmer plot of complex **2** $[Ru(bpy)_2(deeb)]^{2+}$ with ArN_2^+ is shown in Figure 3b. However, instead of a linear relationship of the quencher concentration and lifetime, an exponential behavior is observed. A sphere-of-action model can be adopted to explain this phenomenon.[28] The ET reaction may take place before reactants reach their van der Waals contact distance and may give extra contribution to the reaction. At higher concentrations of the reactants, the sphere-of-action is more pronounced, resulting in increase in the I_o/I factor in an exponential fashion. A modified Stern–Volmer equation (eq 2) is therefore employed to fit the observed data:

$$I_o/I = \tau_o/\tau = (1 + k_q\tau_o[Q])\exp(V[Q]) \quad (2)$$

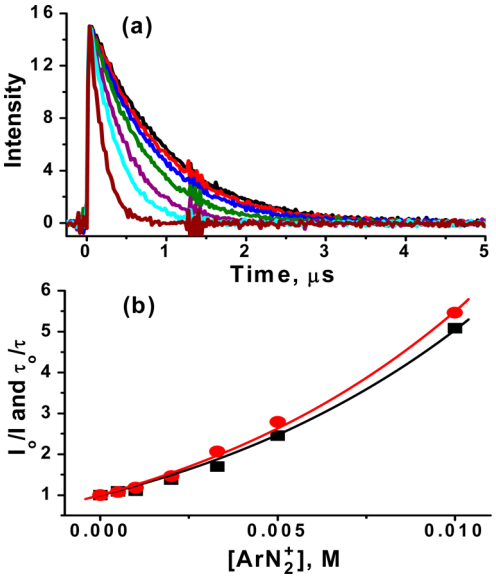

Figure 3. (a) Emission decay observed at 668 nm for complex **2** with various concentrations of ArN_2^+. $[ArN_2^+]$ = 0 (−), 0.5 (red line), 1.0 (dark blue line), 2.0 (green line), 3.3 (purple line), 5.0 (light blue line), and 10.0 (brown line) mM. (b) Stern–Volmer plots for I_o/I (black) and τ_o/τ (red) vs $[ArN_2^+]$. Solid lines are fits obtained from eq 2.

where V is the effective reaction volume. By using τ_o of 910 ns, k_q and V are determined as 1.6×10^8 M^{-1} s^{-1} and 81.1 M^{-1}, respectively. Other complexes show similar behavior, and the calculated effective reaction volume is around ∼80 M^{-1}, which gives the effective reaction radius as around 3.2 nm. Quenching rate constants determined are listed in Table 2.

Transient kinetic measurements of the quenching reaction at MLCT band exhibit ground state bleach recovery. However, the recovery does not complete. For reactions with ArN_2^+, the bleaching region shows a fast partial recovery from the nonreacted excited complexes, and the remaining bleach is held at the same magnitude up to 1 ms. This result indicates that a long-lived intermediate is formed. Considering the nature of the ArN_2^+, the intermediate is attributed to the oxidized form of each ruthenium sensitizer, Ru(III) species. The long-lived character of the Ru(III) species further supports the irreversible nature of the quenching of the excited state of the Ru(II) sensitizer by ArN_2^+. The reactions of ruthenium complexes with ArN_2^+ are summarized in eqs 3–5.

$$Ru^{II} + h\nu \rightarrow Ru^{II*} \quad (3)$$

$$Ru^{II*} + ArN_2^+ \rightarrow Ru^{III} + Ar^{\bullet} + N_2 \quad (4)$$

$$Ar^{\bullet} + \text{solvent} \rightarrow Ar - H \quad (5)$$

Upon reduction, ArN_2^+ quickly releases a nitrogen molecule and an aryl radical. Dinitrogen evolves out of the solution for its low solubility in acetonitrile, and the aryl radical abstracts a hydrogen atom from solvent to produce Ar–H. This photoinduced electron-transfer produces Ru^{3+} species in the solution for at least 1 ms.[29]

Reaction of Ru^{3+} with Br^-. The formation of long-lived Ru^{3+} species gives the possibility to directly observe its reaction with bromide. Mixing 50 μM of complex **2**, 10 mM of ArN_2^+ and various bromide concentrations (50 to 1000 μM) showed no change in the MLCT region of the absorption spectra and

DOI: 10.1021/acs.inorgchem.7b01238
Inorg. Chem. XXXX, XXX, XXX–XXX

Table 2. Bimolecular Quenching Rate Constants, Excited-State Potential Energies and Reduction Potentials, Work Term and Reaction Gibbs Energies of Ruthenium Complexes with ArN_2^+

	$[Ru(LL)]^{2+}$, LL =	k_q, M^{-1} s^{-1}	V, M^{-1}	r,[a] nm	E_{00},[b] eV	$E_{1/2}(Ru^{III/II*})$, V	ΔG_w, eV	$-\Delta G_{ET(q)}$,[c] eV
1	$(bpy)_3$	1.1×10^9	83.0	3.20	2.18	−0.92	0.12	0.70
2	$(bpy)_2(deeb)$	1.6×10^8	81.1	3.18	1.94	−0.58	0.11	0.37
3	$(deeb)_2(dmbpy)$[d]	1.4×10^8	83.5	3.21	1.98	−0.56	0.10	0.36
4	$(deeb)_2(bpy)$	1.2×10^8	74.4	3.09	2.02	−0.56	0.11	0.35
5	$(deeb)_3$	6.4×10^7	84.1	3.22	2.09	−0.53	0.10	0.33
6	$(deeb)_2(bpz)$	8.9×10^6[e]	*f*	*f*	2.05	−0.39	0.12	0.17

[a]Effective reaction radius, determined from volume V. [b]Calculated from the time-dependent DFT method. [c]$-\Delta G_{ET(q)} = -(E_{1/2}(Ru^{III/II*}) - E(ArN_2^{+/0}) + \Delta G_w)$, see text, where $E(ArN_2^{+/0}) = -0.10$ V vs SCE. [d]Ref 21. [e]The emission intensity and lifetime changes with various quencher concentrations are within the instrument limit. The quenching rate constant is estimated from the yields of Ru(III) measured at MLCT bleach spectra. [f]Fits linear Stern−Volmer equation.

maintained the same emission intensities and lifetimes. Although bromide is capable of quenching the excited-state of ruthenium complexes, the quenching-rate constants are in the proximity of $\sim 10^6$ M^{-1} s^{-1}.[21] At the highest bromide concentration of 1 mM, it cannot compete with the quenching reaction of 10 mM of ArN_2^+. Transient kinetics of the three-components solution of complex **2** exhibits a dramatic change at the MLCT bleach region (Figure 4). The long-lived bleach signals recovery back to baseline due to Ru^{3+} reacting with Br^-.

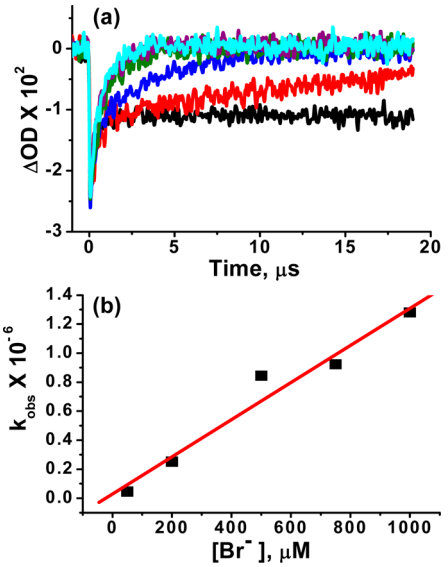

Figure 4. (a) Transient kinetics monitored at 476 nm of 5.0×10^{-5} M of complex **2**, 10 mM of ArN_2^+ and various Br^- concentrations in acetonitrile. $[Br^-]$ = 0 (−), 50 (red line), 200 (dark blue line), 500 (green line), 750 (purple line), and 1000 (light blue line) μM. (b) Plot of observed rate constants vs $[Br^-]$.

Ru^{III} formed from the excited-state quenching is about 1 μM in this reaction condition.[30] With a bromide concentration of at least 50 μM, the slow bleach-recovery signal is treated as a pseudo-first order reaction and is fitted to a single-exponential decay function. By plotting the observed rates vs the bromide concentration, the bimolecular reaction rate constant can be obtained (Figure 4b). Complexes **1**, **3**−**5** show similar kinetics, and the rates are listed in Table 3. Complex **6** has very low quenching to generate a sufficient amount of the corresponding Ru(III) species, and therefore, is not subject to the bromide reaction.

Direct Observation of Products by Transient Absorption. Transient kinetics monitored at 390 nm provide important information about the intermediates and reaction products. Figure 5 exhibits the excited-state absorption of 50 μM of complexes, 10 mM of ArN_2^+, and 1 mM Br^- at 390 nm. Complexes **1** (Figure 5a) and **5** (Figure 5e) show clear biphasic processes. In this reaction condition, the excited-state of complex **1** is completely quenched by ArN_2^+ within 0.5 μs. The observed biphasic kinetics must be due to subsequent reactions. As shown in Figure 5a, the growth rate matches its Ru(III) decay rate monitored at 451 nm; therefore, this growth process is assigned to the bimolecular reaction of Ru(III) with Br^-. The positive signal indicates a new species is formed and absorbs at 390 nm with a larger extinction coefficient than Ru(III) species. After ∼5 μs, the positive signal begins to decay. The decay process is attributed to the reaction of the new species and has been followed to its completion (Figure 5f, black line). Complex **5**, on the other hand, shows two decay kinetics (Figure 5e). Since the calculated reaction rate for the excited-state quenching of complex **5** with ArN_2^+ (6.4×10^5 s^{-1}) is much slower than the calculated reaction rate of Ru(III) with Br^- (1.1×10^7 s^{-1}), the fast decay signal is the excited-state decay, but the rate is dominated by the fast reaction between Ru(III) and Br^-. For complexes **2**−**4**, the two reactions, the oxidative quenching of the excited state by ArN_2^+ and the oxidation of Br^- by Ru(III), have comparable rates within

Table 3. Reaction Rate Constants, Work Term, Gibbs Energies, and Turnover Numbers for Bimolecular Reaction of Photogenerated Ru^{III} Complexes with Bromide

	$[Ru(LL)]^{2+}$, LL =	$k_{ET(Br)}$, M^{-1} s^{-1}	$E_{1/2}(Ru^{III/II})$, V	ΔG_w, eV	$-\Delta G_{ET(Br)}$,[a] eV	TON
1	$(bpy)_3$	1.2×10^8	1.26	−0.15	0.19	116
2	$(bpy)_2(deeb)$	1.3×10^9	1.36	−0.14	0.28	142
3	$(deeb)_2(dmbpy)$[b]	4.0×10^9	1.42	−0.13	0.33	160
4	$(deeb)_2(bpy)$	4.8×10^9	1.46	−0.14	0.38	152
5	$(deeb)_3$	1.1×10^{10}	1.56	−0.13	0.47	140

[a]$-\Delta G_{ET(Br)} = -(E(Br^{\bullet}/Br^-) - E_{1/2}(Ru^{III/II}) + \Delta G_w)$, where $E(Br^{\bullet}/Br^-) = +1.22$ V vs SCE. [b]Ref 21.

DOI: 10.1021/acs.inorgchem.7b01238
Inorg. Chem. XXXX, XXX, XXX−XXX

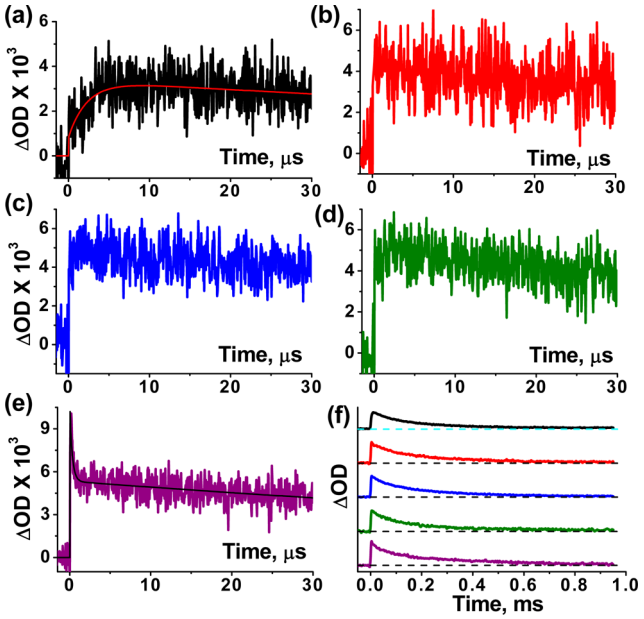

Figure 5. Transient absorption monitored at 390 nm. (a–e) 5.0 × 10^{-5} M of complexes **1**–**5**, 10 mM of ArN_2^+ and 1 mM Br^- in acetonitrile solution. Solid lines are calculated spectra using rate constants listed in Table 3 and $Br_2^{-\bullet}$ disproportionation rate constant of 5 × 10^9 M^{-1} s^{-1}. (f) Same kinetics of (a–e) (top to bottom) recorded to 1 ms.

individual complexes. The kinetics traces in Figure 5b–d exhibit a slight hint of multiphasic behavior.

Notably, the initial rapid process possesses a rate that is sensitive to the choice of complexes among **1**–**5**, while the rates for the slower process in the sub-millisecond time domain is rather insensitive to the choice of complex (Figure 5f). The similarity in the latter slow decay rates supports that the ruthenium species does not participate in the latter slow process. Molar extinction coefficient at 390 nm of bromine related species has been reported for $Br_2^{-\bullet}$, Br_2, and Br_3^- of 3800, 225, and 770 M^{-1} cm^{-1}, respectively,[31,32] The extinction coefficients of Br_2 and Br_3^- are too small to be the major component in the microsecond time range. One-electron oxidation of Br^- should give $Br^\bullet$. It has been reported that $Br^\bullet$ combines with Br^- in diffusion limit to form $Br_2^{-\bullet}$.[31] Therefore, we assign the species formed in the reaction with Ru(III) that absorbs at 390 nm to $Br_2^{-\bullet}$. The slow decay at 390 nm has been fitted to an equal concentration bimolecular reaction with a rate constant of 5 × 10^9 M^{-1} s^{-1}. This reaction is attributed to the disproportionation reaction of $Br_2^{-\bullet}$ to Br_3^- and Br^-. There is a small residue signal at 1 ms for all reactions. Transient absorption indicates the reactions followed by Ru(III) reacts with Br^- are summarized in eqs 6–8.

$$Ru^{III} + Br^- \rightarrow Ru^{II} + Br^{\cdot} \quad (6)$$

$$Br^\bullet + Br^- \xrightarrow{fast} Br_2^{-\bullet} \quad (7)$$

$$Br_2^{-\bullet} + Br_2^{-\bullet} \rightarrow Br_3^- + Br^- \rightleftharpoons Br_2 + 2Br^- \quad (8)$$

Hexene has been routinely utilized to detect bromine.[33] Since Br_3^- and Br^- are in equilibrium with Br_2 + $2Br^-$,[21] the hexene reaction is utilized to confirm the production of Br_3^- and/or Br_2. Steady-state photochemistry has been performed to acquire a suitable amount of product. Deuterated acetonitrile solution of complex **2** with 20 mM of ArN_2^+ and Br^- has been excited at 476 ± 16 nm from a 150 W Xe lamp.[34] When the reaction was completed, 10 mM of 1-hexene was added into the solution. NMR sample was prepared by vacuum distillation of the reaction solution. As shown in Figure 6, ^{1}H NMR spectrum

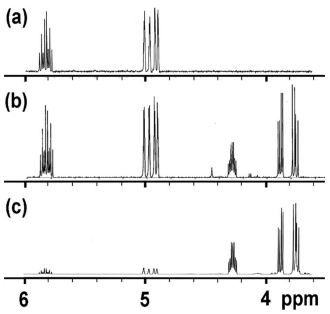

Figure 6. Proton NMR spectra for (a) 1-hexene, (b) 10 mM of 1-hexene reacted with a steady-state photochemical product of 5.0 × 10^{-5} M complex **2**, 20 mM of ArN_2^+, and 20 mM Br^- in acetonitrile-*d* solution, and (c) 10 mM of 1-hexene reacted with Br_2(l).

of the solution from photoreaction exhibits both 1-hexene and 1,2-dibromohexane peaks. From the peak integration of Figure 6b, the TON is obtained as 144.[35] Similar steady-state photochemistry has been performed for other complexes (**1**, **3**–**5**). The TONs obtained are listed in Table 3.

Bimolecular Electron Transfer Reactions. In this study, bimolecular electron transfer reactions are keys to utilize solar energy. Marcus ET theory describes the relationship between ET rates and reaction Gibbs energy.[36] The reaction Gibbs energies for the electronically excited ruthenium complexes and ArN_2^+ are calculated using $\Delta G_{ET(q)} = E_{1/2}(Ru^{III/II*}) - E(ArN_2^{+/0}) + \Delta G_w$, where ΔG_w is the work term that brings two reactants together and is calculated from eq 9.[37]

$$\Delta G_w = \frac{k_e}{\varepsilon}\frac{Z_1 Z_2}{r_{12}} \quad (9)$$

where k_e is Coulomb's constant, ε is the relative permittivity of acetonitrile (37.5), Z_1 and Z_2 are the charges of the reactants, and r_{12} is the van der Waals contact distance for the reactants. The calculated results are listed in Table 2. The reaction Gibbs energies for photogenerated Ru(III) species and bromide are calculated using $\Delta G_{ET(Br)} = E(Br^\bullet/Br^-) - E_{1/2}(Ru^{III/II}) + \Delta G_w$ and are listed in Table 3, where $E(Br^\bullet/Br^-)$ is estimated from ET reactions of +1.22 V vs SCE.[31]

Reaction rate constants for both bimolecular reactions exhibit a positive linear relationship with reaction Gibbs energies. By fitting into classical Marcus electron transfer theory (eq 10),[36] reorganization energies for the reactions are obtained.

$$k_{ET} = \nu_n e^{-(\lambda+\Delta G^\circ)^2/4\lambda k_B T} \quad (10)$$

where ν_n is nuclear motion frequency (10^{13} s^{-1}) and λ is the reorganization energy for the reaction.

As shown in Figure 7, the reorganization energy for the excited-state and quencher reaction (eq 4) is 1.82 eV. The self-exchange reorganization (λ_{11}) of $Ru(bpy)_3^{3+/2+}$ has been reported to be 0.57 eV.[38] By using the Marcus cross-relation ($\lambda_{12} = 1/2\ \lambda_{11} + 1/2\ \lambda_{22}$), the self-exchange reorganization (λ_{22}) for ArN_2^+ is estimated to be 3.07 eV. Since the reaction involves a bond breaking in $ArN_2^{+/0}$, large reorganization energy is expected.[39] This large reorganization energy also explains the smaller rate constants for the excited-state reaction compared

DOI: 10.1021/acs.inorgchem.7b01238
Inorg. Chem. XXXX, XXX, XXX–XXX

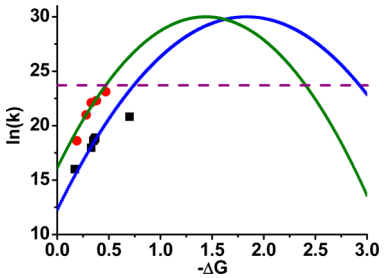

Figure 7. Plot of ET reaction rate constants vs negative Gibbs energy. Black squares: Data from the excited-state quenching reactions. Red circles: Data from the Ru(III) and Br^- reactions. Solid lines are the fits to classical Marcus theory (eq 10). Dash line is the diffusion limit of 2×10^{10} M^{-1} s^{-1}.

to the Ru(III) and Br^- reaction with similar reaction Gibbs energy. Performing the same calculation for Ru(III) and Br^- reaction of λ_{12} = 1.45 eV, we estimate the self-exchange reorganization (λ_{22}) for $Br^{\bullet}/^-$ is 2.33 eV. This value is smaller than that calculated from eq 11 of 2.85 eV.[36,38] This result indicates that bromide is partially solvated in acetonitrile.

$$\lambda_{out} = \Delta e^2\left(\frac{1}{2a_{red}} + \frac{1}{2a_{ox}} - \frac{1}{r}\right)\left(\frac{1}{D_{op}} - \frac{1}{D_s}\right) \quad (11)$$

where Δe is the charge transferred from one reactant to the other, a_{red} and a_{ox} are the diameter of reduced and oxidized species, in this case Br^- (185 pm) and $Br^{\bullet}$ (115 pm), respectively; r is the center-to-center separation distance, D_{op} and D_s are the optical (square of refractive index) and static dielectric constants of the solvent, respectively.

The overall reactions are summarized in Scheme 2. Incorporating bipyridine ligands with electron withdrawing

Scheme 2

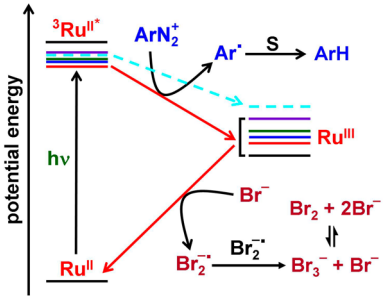

groups alternates both the MLCT excited-state and oxidation potentials for complexes **1**–**6**. The oxidation potentials have bigger changes than the excited-state potential energy changes. While keeping the irradiation in the visible region, the flash-quenched products have 0.4 eV variants. High oxidation potentials of the complexes are essential to oxidize bromide.

Although the quenching rate constants for ruthenium complexes **1**–**5** with ArN_2^+ differ by about 20-fold, 10 mM of ArN_2^+ quenched the excited ruthenium complexes to Ru^{3+} in less than 5 μs. With 1 mM Br^- present, Ru^{3+} completely reacted in about 10 μs. These fast reactions ensure no side reactions that may occur from either ruthenium excited-states or oxidized species. Bimolecular reactions allowed us to adjust the concentrations of each reactant to give reactions in designed sequential steps. Although $Br_2^{-\bullet}$ formed in low concentration, as the only reactive species in the solution, it quantitatively disproportionates to Br_3^- and Br^-.

CONCLUSION

Conversion of solar energy into chemical forms is the central topic of photochemistry. Bimolecular reactions combined with the flash-quench technique ransom part of the photon energy to generate a low concentration reactive species that reacts further with additional high concentration reactants. In this design, part of the photon energy is stored in Br–Br bond formation. The last step for the Br_3^-/Br_2 formation is the slow equal-concentration bimolecular reaction. Since the production of its precursor, $Br_2^{-\bullet}$, consumes the reactive species in solution, the slow reaction can proceed to afford the final product without interference. The photosensitizer, Ru complexes, cycled back to the original state in the ground state within 5 μs.

To achieve high TON, it is important to balance the driving force of *Ru and Ru^{III} reactions. Complex **1** has the highest driving force for excited-state quenching, but it has the lowest driving force for the oxidation of bromide and gives a minimal yield. Complex **6** is prepared to have the highest driving force for the reaction with Br^-. Nevertheless, it shows low efficiency in quenching to generate its strongly oxidizing Ru(III) oxidation state. Complexes **2**–**5** have the best balance that gives satisfied reaction rate constants for both reactions. TON around 150 for complexes **2**–**5** support the argument. Bromine production ultimately results in a drastic increase in optical density leading to loss in the excitation efficiency by the Ru sensitizers. The methodology for the efficient removal of the photogenerated Br_2 during the photolysis must be developed in order to gain a long-term productivity of the system.

ASSOCIATED CONTENT

Supporting Information

The Supporting Information is available free of charge on the ACS Publications website at DOI: 10.1021/acs.inorgchem.7b01238.

General instruments, synthesis, time-dependent DFT method, ^1H NMR spectrum, ESI mass spectrum of complexes **1**–**6**. Quenching experiments, bromide reaction of complexes **1**, **4**, and **5**, hexene reaction with photoproduct of complexes **1**, **3**–**5** (PDF)

AUTHOR INFORMATION

Corresponding Author

*E-mail: changijy@ntnu.edu.tw.

ORCID

I-Jy Chang: 0000-0001-5565-8174

Notes

The authors declare no competing financial interest.

ACKNOWLEDGMENTS

The authors thank Prof. Ming-Kang (Brad) Tsai for his DFT calculation of the excited-state potentials. Financial support from National Taiwan Normal University is acknowledged.

REFERENCES

(1) Fukuzumi, S.; Ohkubo, K.; Suenobu, T. Long-Lived Charge Separation and Applications in Artificial Photosynthesis. *Acc. Chem. Res.* **2014**, *47*, 1455–1464.

DOI: 10.1021/acs.inorgchem.7b01238
Inorg. Chem. XXXX, XXX, XXX–XXX

(2) Kamat, P. V. Meeting the Clean Energy Demand: Nanostructure Architectures for Solar Energy Conversion. *J. Phys. Chem. C* **2007**, *111*, 2834−2860.
(3) Kalyanasundaram, K. Photophysics, Photochemistry and Solar Energy Conversion with Tris(bipyridyl)ruthenium(II) and Its Analogs. *Coord. Chem. Rev.* **1982**, *46*, 159−244.
(4) Takeda, H.; Koike, K.; Inoue, H.; Ishitani, O. Development of an Efficient Photocatalytic System for CO_2 Reduction Using Rhenium(I) Complexes Based on Mechanistic Studies. *J. Am. Chem. Soc.* **2008**, *130*, 2023−2031.
(5) Kuriki, R.; Matsunaga, H.; Nakashima, T.; Wada, K.; Yamakata, A.; Ishitani, O.; Maeda, K. Nature-Inspired, Highly Durable CO_2 Reduction System Consisting of a Binuclear Ruthenium(II) Complex and an Organic Semiconductor Using Visible Light. *J. Am. Chem. Soc.* **2016**, *138*, 5159−5170.
(6) Chang, I.-J.; Gray, H. B.; Winkler, J. R. High-Driving-Force Electron Transfer in Metalloproteins: Intramolecular Oxidation of Ferrocytochrome c by $Ru(2,2'\text{-bpy})_2(im)$ (His-33)$^{3+}$. *J. Am. Chem. Soc.* **1991**, *113*, 7056−7057.
(7) Dempsey, J. L.; Winkler, J. R.; Gray, H. B. Proton-Coupled Electron Flow in Protein Redox Machines. *Chem. Rev.* **2010**, *110*, 7024−7039.
(8) Stemp, E. D. A.; Arkin, M. R.; Barton, J. K. Oxidation of Guanine in DNA by $Ru(phen)_2(dppz)^{3+}$ Using the Flash-Quench Technique. *J. Am. Chem. Soc.* **1997**, *119*, 2921−2925.
(9) Yoo, J.; Delaney, S.; Stemp, E. D. A.; Barton, J. K. Rapid Radical Formation by DNA Charge Transport through Sequences Lacking Intervening Guanines. *J. Am. Chem. Soc.* **2003**, *125*, 6640−6641.
(10) Arnold, A. R.; Barton, J. K. DNA Protection by the Bacterial Ferritin Dps via DNA Charge Transport. *J. Am. Chem. Soc.* **2013**, *135*, 15726−15729.
(11) Esswein, A. J.; Nocera, D. G. Hydrogen Production by Molecular Photocatalysis. *Chem. Rev.* **2007**, *107*, 4022−4047.
(12) Powers, D. C.; Hwang, S. J.; Zheng, S.-L.; Nocera, D. G. Halide-Bridged Binuclear HX-Splitting Catalysts. *Inorg. Chem.* **2014**, *53*, 9122−9128.
(13) O'Regan, B.; Grätzel, M. low-cost, high-efficiency solar cell based on dye-sensitized colloidal TiO_2 films. *Nature* **1991**, *353*, 737−740.
(14) Rowley, J. G.; Farnum, B. H.; Ardo, S.; Meyer, G. J. Iodide Chemistry in Dye-Sensitized Solar Cells: Making and Breaking I-I Bonds for Solar Energy Conversion. *J. Phys. Chem. Lett.* **2010**, *1*, 3132−3140.
(15) Kubiak, C. P.; Schneemeyer, L. F.; Wrighton, M. S. Visible Light Driven Generation of Chlorine and Bromine. Photooxidation of Chloride and Bromide in Aqueous Solution at Illuminated n-Type Semiconducting Molybdenum Diselenide and Molybdenum Disulfide Electrodes. *J. Am. Chem. Soc.* **1980**, *102*, 6898−6900.
(16) Neyhart, G. A.; Marshall, J. L.; Dressick, W. J.; Sullivan, B. P.; Watkins, P. A.; Meyer, T. J. Excited State Photoelectrochemical Production of H_2O_2 and Br_2. *J. Chem. Soc., Chem. Commun.* **1982**, 915−917.
(17) Slama-Schwok, A.; Gershuni, S.; Rabani, J.; Cohen, H.; Meyerstein, D. An Iridium-Bipyridine Complex as a Photosensitizer for the Bromide Oxidation to Bromine by Oxygen. *J. Phys. Chem.* **1985**, *89*, 2460−2464.
(18) Dabestani, R.; Wang, X.; Bard, A. J.; Campion, A.; Fox, M. A.; Webber, S. E.; White, J. M. Photoinduced Oxidation of Bromide to Bromine on Irradiated Platinized TiO_2 Powders and Platinized TiO_2 Particles Supported In Nafion Films. *J. Phys. Chem.* **1986**, *90*, 2729−2732.
(19) Grätzel, M.; Halmann, M. Photosensitized Oxidation of Bromide to Bromine with Phthalic Acid Derivatives in Aqueous Solutions. *Sol. Energy Mater.* **1990**, *20*, 117−129.
(20) Lever, A. B. P. Electrochemical Parametrization of Metal Complex Redox Potentials, Using the Ruthenium(III)/Ruthenium(II) Couple To Generate a Ligand Electrochemical Series. *Inorg. Chem.* **1990**, *29*, 1271−1285.
(21) Tsai, K. Y.-D.; Chang, I.-J. Photocatalytic Oxidation of Bromide to Bromine. *Inorg. Chem.* **2017**, *56*, 693−696.
(22) Ward, W. M.; Farnum, B. H.; Siegler, M.; Meyer, G. J. Chloride Ion-Pairing with Ru(II) Polypyridyl Compounds in Dichloromethane. *J. Phys. Chem. A* **2013**, *117*, 8883−8894.
(23) Bergeron, B. V.; Meyer, G. J. Reductive Electron Transfer Quenching of MLCT Excited States Bound To Nanostructured Metal Oxide Thin Films. *J. Phys. Chem. B* **2003**, *107*, 245−254.
(24) Sun, Y.; Hudson, Z. M.; Rao, Y.; Wang, S. Tuning and Switching MLCT Phosphorescence of $[Ru(bpy)_3]^{2+}$ Complexes with Triarylboranes and Anions. *Inorg. Chem.* **2011**, *50*, 3373−3378.
(25) Farnum, B. H.; Gardner, J. M.; Meyer, G. J. Flash-Quench Technique Employed To Study the One-Electron Reduction of Triiodide in Acetonitrile: Evidence for a Diiodide Reaction Product. *Inorg. Chem.* **2010**, *49*, 10223−10225.
(26) Romain, S.; Leprêtre, J.-C.; Chauvin, J.; Deronzier, A.; Collomb, M. N. Di(μ-oxo) Binuclear Manganese(III,IV) Poly(bipyridyl) Complexes Bearing Four Ruthenium(II) Photoactive Units: Synthesis, Characterization, and Photoinduced Electron-Transfer Properties. *Inorg. Chem.* **2007**, *46*, 2735−2743.
(27) Cano-Yelo, H.; Deronzier, A. Photo-oxidation of Tris(2,2′-bipyridine)ruthenium(II) by *para*-Substituted Benzene Diazonium Salts in Acetonitrile. *J. Chem. Soc., Faraday Trans. 1* **1984**, *80*, 3011−3019.
(28) Pandey, S.; Ali, M.; Bishnoi, A.; Azam, A.; Pandey, S.; Chawla, H. M. Quenching of Pyrene Fluorescence by Calix[4]arene and Calix[4]resorcinarenes. *J. Fluoresc.* **2008**, *18*, 533−539.
(29) No decay in our instrument limit of 1 ms.
(30) Calculated from the MLCT bleach signal and extinction coefficient.
(31) Li, G.; Ward, W. M.; Meyer, G. J. Visible Light Driven Nanosecond Bromide Oxidation by a Ru Complex with Subsequent Br-Br Bond Formation. *J. Am. Chem. Soc.* **2015**, *137*, 8321−8323.
(32) Bianchini, R.; Chiappe, C. Stereoselectivity and Reversibility of Electrophilic Bromine Addition to Bromide-Tribromide-Pentabromide Equilibrium in the Counteranion of the Stilbenes in Chloroform: Influence of the Ionic Intermediates. *J. Org. Chem.* **1992**, *57*, 6474−6478.
(33) Teets, T. S.; Nocera, D. G. Halogen Photoreductive Elimination from Gold(III) Centers. *J. Am. Chem. Soc.* **2009**, *131*, 7411−7420.
(34) The excitation wavelength was selected using monochromator.
(35) From the integration ratio of hexene and dibromohexane and total of 10 mM hexene added, the amount of dibromohexane is calculated to be 3.6 mM. The TON for 50 μM complex **2** is 144.
(36) Marcus, R. A.; Sutin, N. Electron transfers in chemistry and biology. *Biochim. Biophys. Acta, Rev. Bioenerg.* **1985**, *811*, 265−322.
(37) Troian-Gautier, L.; Beauvilliers, E. E.; Swords, W. B.; Meyer, G. J. Redox Active Ion-Paired Excited States Undergo Dynamic Electron Transfer. *J. Am. Chem. Soc.* **2016**, *138*, 16815−16826.
(38) Brown, G. M.; Sutin, N. A Comparison of the Rates of Electron Exchange Reactions of Ammine Complexes of Ruthenium(II) and -(III) with the Predictions of Adiabatic, Outer-Sphere Electron Transfer Models. *J. Am. Chem. Soc.* **1979**, *101*, 883−892.
(39) Lewandowska-Andralojc, A.; Polyansky, D. E. Mechanism of the Quenching of the Tris(bipyridine)ruthenium(II) Emission by Persulfate: Implications for Photoinduced Oxidation Reactions. *J. Phys. Chem. A* **2013**, *117*, 10311−10319.

DOI: 10.1021/acs.inorgchem.7b01238
Inorg. Chem. XXXX, XXX, XXX−XXX